IX-E Field-Effect Transistors with Organic Semiconductors

Considerable attention has recently focused on organic field-effect transistors (OFET) because of their potential use in low-cost flexible electronic devices. We have studied output characteristics of OFET devices based on newly synthesized organic compounds.

IX-E-1 Field-Effect Transistors Based on Dicyanopyrazinoquinoxaline Derivatives

NISHIDA, Jun-ichi[1]; NARASO[1]; MURAI, Shiro[1]; FUJIWARA, Eiichi; TADA, Hirokazu; TOMURA, Masaaki; YAMASHITA, Yoshiro[1]
([1]Tokyo Inst. Tech.)

[*Org. Lett.* **6**, 2007–2010 (2004)]

Dicyanopyrazinoquinoxaline derivatives (Figure 1) have been prepared and characterized by using single-crystal X-ray structure analysis and redox potential measurements. They have strong electron-accepting properties due to the pyrazinopyrazine skeletons as well as the cyano groups. Substituents can be easily introduced at the benzene ring and control the HOMO-LUMO energy gap and the molecular packing. Figure 2 shows output characteristics of a bottom-contact OFET based on compound 1a. It was found that the compound **1a** exhibited *n*-type semiconducting behavior with carrier mobility of 3.6×10^{-6} cm^2/Vs. The compounds examined operated as N-type OFETs. The mobility and on/off ratio of the devices are summarized in Table 1.

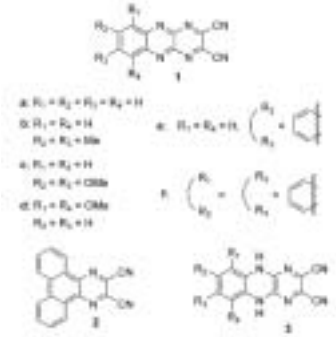

Figure 1. Molecular structures of dicyanopyrazinoquinoxaline derivatives.

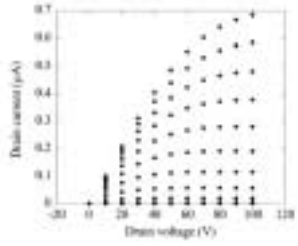

Figure 2. Output characteristics of the OFET based on compound **1a**. Gate voltages were varied from 0 to 100 V with an increment of 10 V.

Table 1. Field-effect mobilities and on/off current ratios of FETs based on dicyanopyrazinoquinoxaline derivatives.

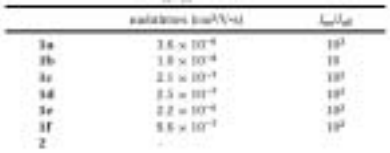

IX-E-2 Low-Voltage Organic Field-Effect Transistors Based on Ta_2O_5 as Gate Insulator Material

SAKAI, Heisuke[1]; FURUKAWA, Yukio[1]; FUJIWARA, Eiichi; TADA, Hirokazu
([1]Waseda Univ.)

[*Chem. Lett.* in press]

A thin film of Ta_2O_5 was prepared by sputtering on heavily-doped silicon substrates and used as a gate insulator of field-effect transistors. Poly(2-methoxy-5-(2'-ethylhexyloxy)-1,4-phenylenevinylene) (MEH-PPV) and pentacene were used as active semiconductors. Interdigital Au electrodes, which consisted of 25 pairs with 25 μm in spacing, 4 mm in width, and 50 nm in thickness, were prepared on the organic layer and used as the source and drain electrodes. Clear saturation in drain currents was observed at low drive voltage of about –3 V as shown in Figure 1. MEH-PPV and pentacence exhibited *p*-type semiconducting behaviors with mobilities of 4.6×10^{-4} cm^2/V s and 0.8 cm^2/V s, respectively.

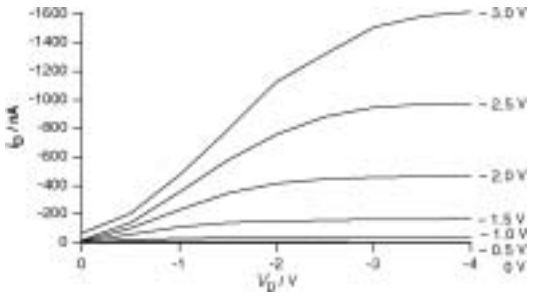

Figure 1. Output characteristics of an FET based on MEH-PPV with a Ta_2O_5 gate insulator.

IX-E-3 Visible Light Emission from Polymer-Based Field-Effect Transistors

SAKANOUE, Tomo[1]; FUJIWARA, Eiichi; YAMADA, Ryo; TADA, Hirokazu
([1]GUAS)

[*Appl. Phys. Lett.* **84**, 3037–3039 (2004)]

Field-effect transistors (FETs) based on poly [2-methoxy, 5-(2'-ethyl-hexoxy)-1,4-phenylenevinylene] (MEH-PPV) were prepared with bottom-contact type interdigital electrodes of Cr/Au and Al/Au on the SiO_2/Si substrates. MEH-PPV exhibited a *p*-type semiconducting behavior and orange light emission was observed when the devices were operated in vacuum. It was found that the luminescence efficiency of the FETs with Al/Au electrodes was higher than that of Cr/Au electrodes, as shown in Figure 1. The simultaneous injection of holes and electrons into MEH-PPV occurred efficiently with the application of Al/Au heteroelectrodes.

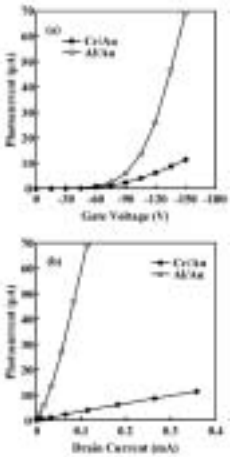

Figure 1. Luminescence intensity detected with a Si photodiode as a function of the gate voltage (a) and the drain current (b). The drain voltage was set at –150 V.

IX-F Molecular Assemblies on Silicon Surfaces *via* Silicon–Carbon Covalent Bonds

Preparation of molecular assemblies on inorganic semiconductors such as silicon and germanium has received a growing interest because of their potential application to stable regist for nano-patterning. We have prepared organic monolayers on silicon by wet process and studied film structures with IR and AFM.

IX-F-1 Temperature Dependence of the Structure of Alkyl Monolayers on Si(111) Surface *via* Si–C Bond by ATR-FT-IR Spectroscopy

YAMADA, Ryo; ARA, Masato[1]; TADA, Hirokazu
([1]GUAS)

[*Chem. Lett*. **33**, 492–493 (2004)]

The temperature dependence of C–H stretching modes of alkyl monolayer formed on Si(111) surface was investigated by an attenuated total reflection Fourier transform infrared spectroscopy from room temperature up to 540 K. Continuous disordering of the monolayer was indicated from the gradual peak shifts toward higher frequency in C–H stretch modes upon heating. The irreversible conformational disorder was introduced in the monolayer above 440 K.

IX-F-2 Non-Contact Atomic Force Microscopy Using Silicon Cantilevers Covered with Organic Monolayers *via* Silicon–Carbon Covalent Bonds

ARA, Masato[1]; SASAHARA, Akira[2]; OHNISHI, Hiroshi[2]; TADA, Hirokazu
([1]GUAS; [2]KAST)

[*Nanotechnology* **15**, S65–S68 (2004)]

Silicon cantilevers covered with dodecyl monolayers anchored *via* silicon–carbon covalent bonds were prepared by a wet process and used for non-contact atomic force microscopy (NC-AFM) of TiO_2(110)–(1×1) surfaces. Figure 1 shows an AFM image of the surface taken with the dodecyl-coated cantilevers. Clear images of atomic rows on atomically flat terraces were observed when the substrate was biased around 2.0 V with respect to the cantilevers. The bias voltage required to give clear images for alkyl-coated cantilevers was higher than that for uncoated ones. Since the cantilevers are thermally and chemically stable, they are applicable to various force microscopy to distinguish chemical species on surfaces.

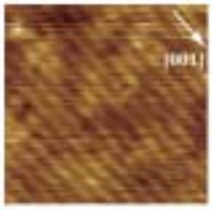

Figure 1. NC-AFM image of the TiO_2 surface (10 nm × 10 nm). The frequency shift and sample bias voltage were set at –186 Hz and 2 V, respectively.

IX-G Low Temperature Scanning Tunneling Microscopy and Spectroscopy of Organic Molecules on Metal Surfaces

The electronic structure of molecules adsorbed by metal surfaces is of growing interest in the field not only of surface science but also of molecular-scale electronic devices. Scanning tunneling microscopy and spectroscopy are powerful tool to investigate molecular arrangements and electronic structure with atomic resolution. We have prepared epitaxial films of phathalocyanine molecules on clean metal surfaces and studies there structures by scanning tunneling microscopy and spectroscopy at low temperature.

IX-G-1 Low Temperature Scanning Tunneling Microscopy of Phthalocyanine Multilayers on Au(111) Surfaces

TAKADA, Masaki[1]; TADA, Hirokazu
([1]GUAS)

[*Chem. Phys. Lett.* **392**, 265–269 (2004)]

We have studied epitaxial trilayer films of cobalt-phthalocyanine (CoPc) on Au(111)-22×√3 surfaces using a scanning tunneling microscope at 78 K. Figure 1 shows an STM image of a CoPc monoleyer on the Au(111) surface. Molecules in each layer were found to form square lattices and stacked along the [1$\bar{1}$0] axis of the Au(111) surface. While CoPc molecules in the first layer were observed at bias voltages of –2.5 to +2.5 V, there were certain ranges of bias voltage in which molecules in the upper layers were invisible. The electronic structures of molecules in upper layers are more localized than those of the first layer, which is affected by the substrate surface.

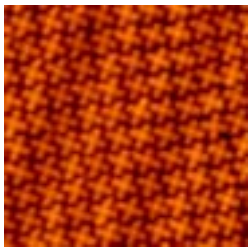

Figure 1. STM image of CoPc molecules on the Au(111) surface (14.6 nm × 14.6 nm).

IX-H Development of New Transport Mechanism Based on Wetting Gradients

Construction and control of wetting gradients on surfaces are of growing interest since the spatiotemporal control of wetting leads to non-mechanical pumping systems in micro-fluidic devices. The imbalance of surface tensions is known to play an important role in the movement of droplets on surfaces. We have succeeded in the reversible control of the direction, magnitude and position of the wetting gradient by in-plane regulation of the electrochemical potential of the thin-film substrate covered with a redox-active self-assembled monolayer. A small droplet of organic liquid was shown to move under the cyclic shift of wetting gradient in aqueous solutions.

IX-H-1 Electrochemically Generated Wetting Gradient and Its Application for the Transport of Droplets

YAMADA, Ryo; TADA, Hirokazu

The in-plane voltage (V_{bias}) was applied to the gold thin film substrate covered with 11-Ferrocenyl-1-undecanethiol (FcC11SH) in addition to the conventional potentiostatic regulation of the potential of the substrate with respect to the reference electrode (RE) (Figure 1a). The current flowing through the substrate causes a continuous potential drop in it. The surface covered with FcC11SH monolayer is known to be hydrophobic and hydrophilic when Fc is reduced and oxidized, respectively. When the potential in the substrate crosses the oxidation potential of the FcC11 HS monolayer, a gradient in the extent of oxidation of the ferrocene, and thus, the wetting across the surface is generated (Figure 1b). The generation and regulation of wetting gradient by this method was confirmed by observing the shape of three droplets of nitrobenzene aligned in the biased direction. The one (Figure 2a; left was more negative) and two (Figure 2b) of the droplets got wet as the V_{bias} was increased. Since the electrochemical reaction of ferrocene is reversible, the observed wetting transition was reversible. Position of the wetting gradient can be moved by E_{offset} and direction and magnitude of it are controlled by V_{bias} in Figure 1a. The spatiotemporal control of the wetting gradient enabled us to manipulate a droplet on a substrate. Figure 3 shows the droplet moved in inchworm-like manner. Initially, the wetting gradient was positioned in the left of the picture and the left side of the substrate was wetting in Figure 3a. As wetting region reached the droplet, droplet spread into left, *i.e.*, wetting area as

shown in Figure 3b. When the position of the wetting gradient was reversed, the droplet shrunk from the right side in Figure 3c. As a result, a net transport of the droplet took place.

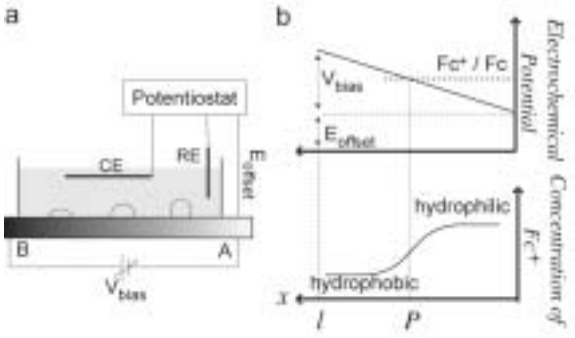

Figure 1. (a) Schematic drawing of the experimental configuration. (b) Potential profile and wetting distribution on the substrate under the biased condition.

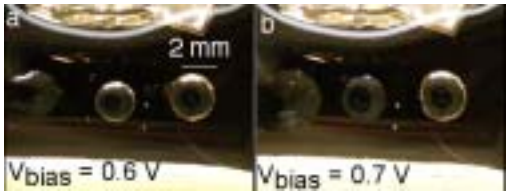

Figure 2. The formation of the wetting gradient by V_{bias}. V_{bias} was –0.6 V(a) and –0.7 V (b). E_{offset} was –300 mV *vs.* AuO_x.

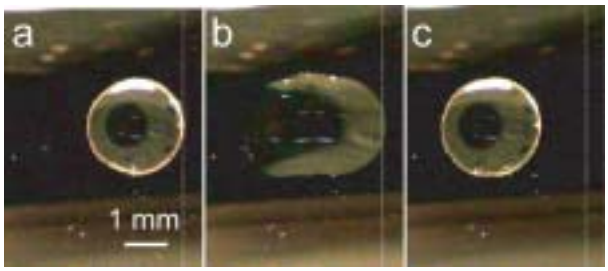

Figure 3. Inchworm motion of the droplet in the solution. See text for details. E_{offset} = (a) –300 mV, (b) –340 mV and (c) –300 mV.